arXiv:1401.1586v2 [cond-mat.str-el] 15 Jan 2014

Strongly fluctuating fermionic superfluid in attractive π-flux Hubbard model

Ya-Jie Wu,[1] Jiang Zhou,[1] and Su-Peng Kou[1,*]

[1]*Department of Physics, Beijing Normal University, Beijing 100875, China*

Ultracold atoms in optical lattice provides a platform to realize the superfluid (SF) state, a quantum order with paired charge-neutral fermions. In this paper, we studied SF state in the two-dimensional attractive Hubbard model with π-flux on each plaquette. The SF state in the π-flux lattice model suffers very strong quantum fluctuations and the ground state becomes a possible *quantum phase liquid* state. In this phase, there exists the Cooper pairing together with a finite energy gap for the atoms, but no long range SF phase coherence exists at zero temperature. In addition, we discussed the properties of the SF vortices.

PACS number(s): 03.75.Ss, 67.85.Lm, 37.10.Jk

I. INTRODUCTION AND MOTIVATION

Using ultracold atoms that form Bose-Einstein Condensates (BEC) or Fermi degenerate gases to do precise measurements and simulations of quantum many-body systems, is quite impressive and has become a rapidly-developing field[1, 2]. Since ultracold atoms may be trapped in optical lattices, together with tunable interaction via Feshbach resonance technique[3, 4], there is a new playground to manipulate a quantum many-body system with unprecedented accuracy. In particular, an extreme physical limit can be reached that is beyond the condition in the condensed matter physics. Recently, using Raman-assisted tunneling in an optical lattice of cold atoms, a large tunable (staggered) magnetic field was realized in experiments[5–7]. The synthetic gauge field enlarges the versatility of the use of ultracold atoms very much, allowing exploring new types of quantum states. In Ref.[8], Zhai *et al* studied the superfluid (SF) on a square lattice with a uniform magnetic flux $2\pi p/q$ (p and q are co-prime integer numbers) on each plaquette, and found that with considering the magnetic translation symmetry of the mean field ansatz, the Cooper pairs may have finite momenta.

For a special artificial staggered gauge field in a square lattice with time reversal symmetry and translation symmetry, there is a π-flux on each plaquette. See the illustration in Fig.1. Namely, due to the nontrivial Aharonov–Bohm phases, the atoms will obtain an extra minus sign after moving around each plaquette. When one considers the attractive interaction between atoms in a π-flux lattice model, the ground state can be an SF. An interesting issue arises "*whether the SF in π-flux lattice model has exotic quantum properties beyond the conventional SF in a square lattice without π-flux*?"

In this paper we will study this issue. We find that the SF in the π-flux lattice model suffers quite strong quantum fluctuations. The strongly fluctuating SF state possesses exotic quantum orders and cannot be described by Landau's symmetry breaking theory. We call it *quantum phase liquid* (QPL) state. In QPL state, the fermions are paired as

$$\left\langle \left| \hat{c}^{\dagger}_{i\uparrow} \hat{c}^{\dagger}_{i\downarrow} \right| \right\rangle = \left\langle \left| \Delta_0 e^{i\phi_i} \right| \right\rangle = |\Delta_0| \neq 0. \tag{1}$$

And the single quasi-particle's excitation has a finite energy gap. However, due to strong quantum fluctuations, the system has no coherence, or the correlation length is finite. Hence, although the amplitude of the SF order parameter is finite, the SF order parameter is zero, i.e.,

$$\langle \hat{c}^{\dagger}_{i\uparrow} \hat{c}^{\dagger}_{i\downarrow} \rangle = \left\langle \Delta_0 e^{i\phi_i} \right\rangle = |\Delta_0| \left\langle e^{i\phi_i} \right\rangle = 0 \tag{2}$$

with considering the random phase ($\phi_i \neq$ constant) of the SF order in the QPL phase. At finite temperature, QPL state becomes a fermionic system with pseudo-energy-gap. However, the fermionic SF vortex in QPL has different topological properties with pseudo-energy-gap at finite temperature, of which the SF vortex always obeys bosonic statistics.

The reminder of this paper is organized as follows. In Sec. II, we write down the π-flux attractive Hubbard model with a Zeeman field on square optical lattice. Then, in Sec. III, we discuss the global symmetry of the system and show the relationship between the attractive model and the repulsive one. In Sec. IV, we

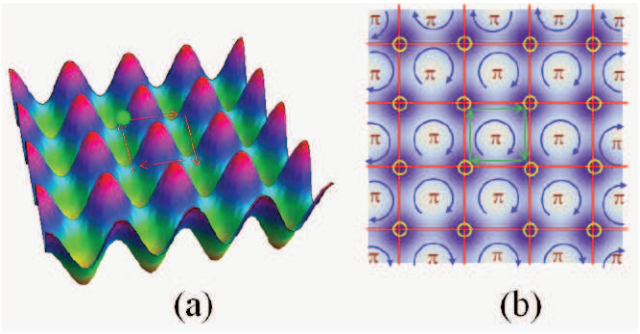

FIG. 1: (Color online) (a) The illustration of potential of the two dimensional optical lattice; (b) Hopping processes encircling a square plaquette acquire an accumulated phase π. The background is contour plot of the optical potential in (a).

*Corresponding author; Electronic address: spkou@bnu.edu.cn

obtain the phase diagram of the attractive model by the mean field approach. In Sec. V, we investigate the phase fluctuations by using random-phase-approximation (RPA) approach and obtain the dispersion of the collective modes. In Sec. VI, we use the nonlinear σ model (NLσM) method to derive the global phase diagram, and we find the QPL state in the global phase diagram. In Sec. VII, we discuss the SF vortex and find that the SF vortex in QPL state can be a fermionic excitation. Finally, we conclude our discussions in Sec. VIII.

II. THE ATTRACTIVE HUBBARD MODEL IN A π-FLUX SQUARE LATTICE

Our starting point is the attractive Hubbard model on a π-flux square lattice, of which the Hamiltonian is

$$\hat{H} = -\sum_{\langle i,j\rangle,\sigma}(t_{ij}\hat{c}^{\dagger}_{i,\sigma}\hat{c}_{j,\sigma} + h.c.) - U\sum_{i}\hat{n}_{i\uparrow}\hat{n}_{i\downarrow} - \mu\sum_{i,\sigma}\hat{c}^{\dagger}_{i\sigma}\hat{c}_{i\sigma} - h\sum_{i,\sigma,\sigma'}\hat{c}^{\dagger}_{i\sigma}\sigma^{z}_{\sigma\sigma'}\hat{c}_{i\sigma'}. \quad (3)$$

Here, $i = (i_x, i_y)$ labels the lattice sites, and $\langle i,j\rangle$ represents all nearest neighboring bonds. In a π-flux lattice as shown in Fig.1, taking the Landau gauge as example, the hopping parameters are $t_{i,i+\hat{e}_x} = t$ if $\langle i,j\rangle$ is along x-direction and $t_{i,i+\hat{e}_y} = (-1)^{i_x}t$ if $\langle i,j\rangle$ is along y-direction[8]. $\sigma,\sigma' = \uparrow,\downarrow$ are spin-indices, U is the strength of the attractive interaction, μ is the chemical potential, and h is the strength of the Zeeman field. In the following parts, we consider the case with $\mu = -U/2$ and take the lattice constant a equal to unity.

III. GLOBAL SYMMETRY

Firstly, we discuss the global symmetry and the spontaneous symmetry breaking of the original Hamiltonian in Eq.(3). The Hamiltonian in Eq.(3) has an SU(2) particle-hole (pseudo-spin) symmetry group, in which the SU(2) group elements act on the space of the SF/CDW order parameters. To make the SU(2) pseudo-spin symmetry clearer, we note that in terms of the canonical particle-hole transformation[9]

$$\hat{c}_{i,\uparrow} \to \tilde{c}^{\dagger}_{i,\uparrow}, \hat{c}_{i,\downarrow} \to (-1)^{i_x+i_y}\tilde{c}^{\dagger}_{i,\downarrow}, \quad (4)$$

the original model is mapped onto that of a repulsive π-flux model with the effective chemical potential $h + U/2$. See Appendix A for the details. Then we can define an SU(2) pseudo-spin symmetry of the Hamiltonian in Eq.(3), i.e.,

$$\hat{H} \to \hat{H}' = \mathcal{U}\hat{H}\mathcal{U}^{-1} = \hat{H} \quad (5)$$

by doing a pseudo-spin rotation $\Psi \to \Psi' = \mathcal{U}\Psi$, with $\Psi = (\tilde{c}_{i,\uparrow}, \tilde{c}_{i,\downarrow})^T$. The SU(2) pseudo-spin operators of the attractive π-flux Hubbard model thus become

$$\begin{aligned}\hat{\eta}^{-}_i &\leftrightarrow (-1)^{i_x+i_y}\hat{\Delta}_i = (-1)^{i_x+i_y}\hat{c}_{i,\downarrow}\hat{c}_{i,\uparrow},\\ \hat{\eta}^{+}_i &\leftrightarrow (-1)^{i_x+i_y}\hat{\Delta}^{\dagger}_i = (-1)^{i_x+i_y}\hat{c}^{\dagger}_{i,\uparrow}\hat{c}^{\dagger}_{i,\downarrow},\\ \hat{\eta}^{z}_i &\leftrightarrow (\hat{\rho}_i - 1)/2,\end{aligned} \quad (6)$$

where $\hat{\eta}^{\pm}_i = \hat{\eta}^{x}_i \pm i\hat{\eta}^{y}_i$, and $\hat{\rho}_i$ is the particle density operator. One may check the SU(2) algebraic relation between the SU(2) pseudo-spin operators as

$$[\hat{\eta}^{\alpha}_i, \hat{\eta}^{\beta}_i] = i\epsilon_{\alpha\beta\gamma}\hat{\eta}^{\gamma}_i \quad (7)$$

with $\epsilon_{\alpha\beta\gamma}$ being antisymmetric tensor. Due to the SU(2) pseudo-spin rotation symmetry, the ground state of the Hamiltonian in Eq.(3) can also be a charge density wave (CDW) state as $\langle\hat{\eta}^{z}\rangle \neq 0$.

For a conventional SF order from spontaneous U(1) phase symmetry breaking, there exists one Goldstone mode due to the quantum phase fluctuation. In two dimensions, there is a Kosterlitz-Thouless (KT) transition, below which the (quasi-) long range phase coherence establishes. Now we have an SF/CDW order from spontaneous SU(2) pseudo-spin rotation symmetry breaking. The quantum fluctuations around the mean field ground state are much stronger. In the CDW order one has nonzero particle density modulation at different sublattices $\langle\hat{\eta}^{z}\rangle \neq 0$. From the commutation relation between the phase ϕ_i of Δ_i and the particle density operator $\hat{\rho}_i$, i.e., $[\phi_i, \hat{\rho}_i] \neq 0$, the nonzero particle density modulation leads to an uncertainty for the SF phase coherence and even destroys the long range SF phase coherence. Thus, the non-zero value of Δ_0 only means the existence of Cooper pairing. It does not necessarily imply that the ground state is a long range SF order. As a result, one needs to examine the stability of SF order against quantum fluctuations based on a formulation by keeping SU(2) pseudo-spin rotation symmetry.

IV. MEAN FIELD CALCULATION

For the attractive π-flux Hubbard model described by Eq.(3), with increasing the interaction strength, the ground state turns into an SF order. Due to the existence of π-flux on each plaquette, we need to consider all Cooper channels including zero momentum paring $\mathbf{q} = (0,0)$ and non-zero momentum paring $\mathbf{q} = (0,\pi)$. From Ref.[8], the order parameter is written as

$$\Delta_i = \sum_{n=0}^{1}\Delta^{n}_{i_x(\mathrm{mod}\,2)}e^{i\pi l i_y}. \quad (8)$$

Here $\Delta^{n}_{i_x(\mathrm{mod}\,2)}$ is the SF order with paring momentum $\mathbf{q} = (0,\pi n)$ on sublattice site $i_x(\mathrm{mod}\,2)$. For instance, sublattice A refers to $i_x(\mathrm{mod}\,2) = 1$ and B refers to $i_x(\mathrm{mod}\,2) = 0$. The explicit form of the order parameters is given by $\Delta_{i\in A,o} = \Delta_{i\in B,o} = a - ib$, and

$\Delta_{i\in A,e} = \Delta_{i\in B,e} = a + ib$, where the subscripts o and e correspond to odd rows and even rows of the π-flux lattice, respectively.

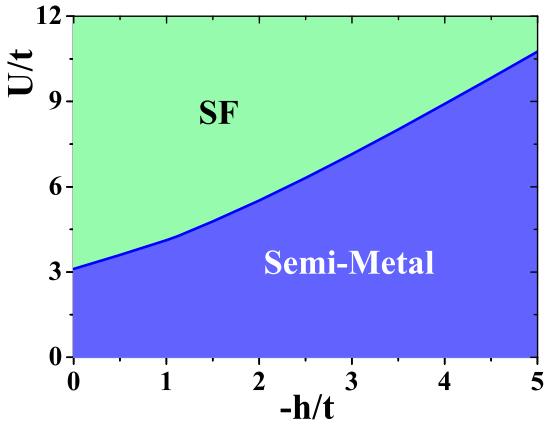

FIG. 2: (Color online) Mean-field phase diagram of the attractive π-flux Hubbard model without considering phase fluctuations at zero temperature. There are two phases: semi-metal (blue region), superfluid (green region).

By the numerical calculations, we find $b = 0$ and the SF order parameter is uniform, i.e., $\Delta_i = a = \Delta_0/2$. Then, by minimizing the free energy F with respect to Δ_0, we obtain the gap equation

$$\frac{1}{U} = \frac{1}{4N_s} \sum_{\alpha, E_{\alpha,\mathbf{k}} > -h} \frac{1}{E_{\alpha,\mathbf{k}}} \tanh\left(\frac{\beta E_{\alpha,\mathbf{k}}}{2}\right), \qquad (9)$$

where the energy spectra are

$$E_{\alpha,\mathbf{k}} = \sqrt{\xi_{\alpha,k}^2 + \left(m_0^{HS}\right)^2}, \qquad (10)$$

with $\xi_{\alpha=\pm,\mathbf{k}} = 2t\sqrt{[\cos^2(k_x) + \cos^2(k_y)]} \pm \mu$ and $m_0^{HS} = U\Delta_0/2$, β is given by $\beta = 1/(k_B T)$ with k_B ($k_B \equiv 1$) the Boltzmann constant and T the temperature, and N_s is the number of the unit cells. The summation is restricted in the reduced Brillouin zone where the relation $E_{\mathbf{k}} > -h$ is satisfied. By solving the mean field equations, we plot the phase diagram in Fig.2 at zero temperature. The blue line in Fig.2 separates the gapped SF order and the semi-metal. In this paper, the chemical potential is fixed as $\mu = -U/2$. We may identify the particle-filling-number n_f by $n_f = -\frac{1}{2N_s}(\frac{\partial F}{\partial \mu})$. The particle-filling-number changes as variation of the chemical potential μ (or interaction U). For example, for the case of $h = 0$, we plot n_f versus the chemical potential μ in Fig.3. By this mean field theory, we can also get a finite SF transition temperature T^* corresponding to the temperature breaking the Cooper pair. In general, this SF transition temperature is high. For example, for the case of $h = -0.1t$, $U = 4t$, the SF transition temperature is $T^* = 0.75t$.

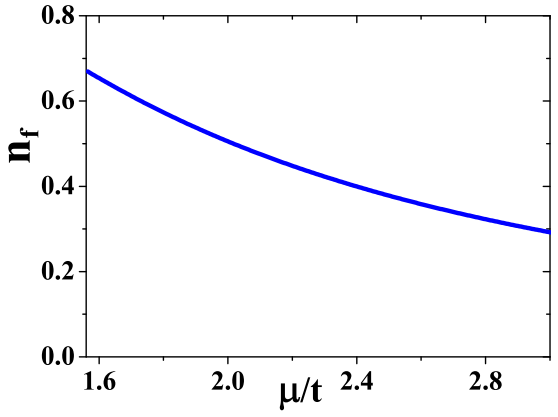

FIG. 3: (Color online) The illustration of particle-filling-number n_f versus the chemical potential μ for the case of Zeeman field $h = 0$.

V. PHASE FLUCTUATIONS BY RANDOM-PHASE-APPROXIMATION APPROACH

To study the quantum fluctuations of the SF/CDW order, firstly we use the random-phase-approximation (RPA) approach to derive the dispersion of the collective modes[10].

In the imaginary-time functional integration formalism, we set $\beta = 1/T$, $\hbar = k_B = 1$. The partition function is then written as

$$Z = \int D\left[c^\dagger, c\right] e^{-S},$$

where the effective action S is

$$S = \int_0^\beta d\tau \left[\sum_{n,\mathbf{k},\sigma} c^\dagger_{n,\mathbf{k},\sigma}(\tau)\, \partial_\tau c_{n,\mathbf{k},\sigma}(\tau) + H(\tau)\right], \qquad (11)$$

where the term $H(\tau)$ can be readily obtained by replacing the femionic operator $\hat{c}_{n,\mathbf{k},\sigma}$ by the Grassman number $c_{n,\mathbf{k},\sigma}$.

By the Hubbard-Stratanovich transformation, the interaction term becomes $e^{-S_{att}}$, where S_{att} is

$$\begin{aligned} S_{att} = \int_0^\beta d\tau \sum_{n,\mathbf{q},\mathbf{k}} & [\tilde{\Delta}_{n,\mathbf{q}}(\tau)\, c^\dagger_{n,\mathbf{k}+\frac{\mathbf{q}}{2},\uparrow}(\tau)\, c^\dagger_{n,-\mathbf{k}+\frac{\mathbf{q}}{2},\downarrow}(\tau) \\ & + \tilde{\Delta}^*_{n,\mathbf{q}}(\tau)\, c_{n,-\mathbf{k}+\frac{\mathbf{q}}{2},\downarrow}(\tau)\, c_{n,\mathbf{k}+\frac{\mathbf{q}}{2},\uparrow}(\tau) \\ & + \frac{N_s}{U} \sum_{n,\mathbf{q}} \tilde{\Delta}^*_{n,\mathbf{q}}(\tau)\, \tilde{\Delta}_{n,\mathbf{q}}(\tau)]. \end{aligned} \qquad (12)$$

Performing an integration over the fermionic field, we have

$$S = \sum_{n,k}(-i\omega_l - \mu) + \frac{N_s}{U}\sum_{n,q} \tilde{\Delta}^*_{n,q}\tilde{\Delta}_{n,q} - tr\left[\ln\left(-G^{-1}\right)\right], \qquad (13)$$

where $i\omega_l = i\omega_l' + h$ with $\omega_l' = (2l+1)\pi/\beta$, and the inverse of the Green function is given by

$$G^{-1} = i\omega_l \mathbb{I} + \begin{pmatrix} -y_{\mathbf{k}}+\mu & x_{\mathbf{k}} & -\tilde{\Delta}_{A,q} & 0 \\ x_{\mathbf{k}} & y_{\mathbf{k}}+\mu & 0 & -\tilde{\Delta}_{B,q} \\ -\tilde{\Delta}^*_{A,q} & 0 & y_{\mathbf{k}}-\mu & -x_{\mathbf{k}} \\ 0 & -\tilde{\Delta}^*_{B,q} & -x_{\mathbf{k}} & -y_{\mathbf{k}}-\mu \end{pmatrix}, \tag{14}$$

where $\mathbb{I}$ is 4×4 identity matrix, the subscripts $n = A, B$ describe two sublattices, and $x_{\mathbf{k}} = 2t\cos k_x$, $y_{\mathbf{k}} = 2t\cos k_y$ (The lattice constant is defined as $a \equiv 1$).

We split the $\tilde{\Delta}_{n,q}$ into a time-independent (stationary) part (that is the mean field value) $\tilde{\Delta}_{n,0}$ and time-dependent part (that represents the phase fluatuations) $\Lambda_n(q)$ as

$$\tilde{\Delta}_{n,q} = \tilde{\Delta}_{n,0}\delta_{q,0} + \Lambda_n(q), \tag{15}$$

where $q = (\mathbf{q}, i\upsilon_l)$ with $\upsilon_l = 2l\pi/\beta$. Then the Green function shown in Eq.(14) can be described by

$$G^{-1} = G_0^{-1} + G_1^{-1}, \tag{16}$$

where $G_0^{-1}(k,k)$ describing the saddle point inverse Nambu matrix takes the form as

$$G_0^{-1} = G^{-1}(\tilde{\Delta}^*_{A,q} \to \tilde{\Delta}_{A,0}, \tilde{\Delta}_{B,q} \to \tilde{\Delta}_{B,0}). \tag{17}$$

In the mean-field approach, the order parameters are $\tilde{\Delta}_{A,0} = \tilde{\Delta}_{B,0} = -m_0^{HS}$.

Expanding the term $tr\left[\ln\left(-G^{-1}\right)\right]$ by using the Taylor formula up to the second order term, the effective action S then becomes $S = S_0 + S_2$, where the zeroth order effective action is

$$S_0 = \sum_{n,k}(-i\omega_l - \mu) + \frac{N_s}{U}\sum_{n,q}\tilde{\Delta}^*_{n,q}\tilde{\Delta}_{n,q} - tr\ln\left(-G_0^{-1}\right), \tag{18}$$

and the second order effective action is

$$S_2 = \frac{1}{2}tr\left[G_0(k+q)\left(G_1^{-1}\right)_{k+q,k}G_0(k)\left(G_1^{-1}\right)_{k,k+q}\right]. \tag{19}$$

Then an effective action $\bar{S}_{flu}$ of quantum fluctuations $\Lambda_n(q)$ becomes

$$\bar{S}_{flu} = \frac{\beta}{2}\sum_q \Lambda^\dagger(q)\,\Pi(q)\,\Lambda(q) = S_2 + g\mathbb{I}, \tag{20}$$

with $\Lambda^\dagger(q) = \left(\Lambda^*_{A,q}\ \ \Lambda_{A,-q}\ \ \Lambda_{B,-q}\ \ \Lambda^*_{B,q}\right)$.

Next, we make use of the Matsubara summation formula to derive the explicit form of $\Pi(q)$. For each element of the function $\Pi_{ij}(q)$, we may write it as the summation of $\Pi_{ij}^{qp-qp}(q)$ and $\Pi_{ij}^{qp-qh}(q)$, where $\Pi^{qp-qp}(q)$ ($\Pi^{qp-qh}(q)$) is the contribution term from the scattering between the quasi-particles and the quasi-particles (the quasi-holes). In order to obtain the pair correlation function (amplitude correlation function and phase fluctuation function), we may first express the fluctuations of the order parameter as

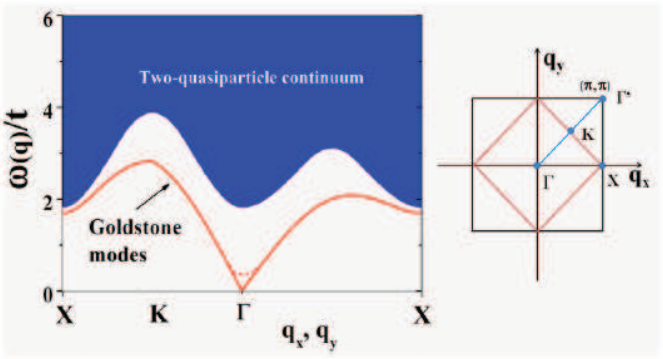

FIG. 4: (Color online) The illustration of collective modes of SF/SDW order for the case of $U/t = 4.0$, $h = 0.0$. The red line corresponds to the Goldstone modes. The blue region denotes two-quasiparticle continuum. The Leggett modes merge into the two-quasiparticle continuum. The red dotted line denotes a dispersion of the Goldstone modes with a small energy gap obtained from the results of O(3) nonlinear σ model by renormalization-group approach.

$$\Lambda_n(q) = \eta_n(q)\,e^{i\phi_n(q)} = \left[\lambda_n(q) + i\theta_n(q)\right]/\sqrt{2}. \tag{21}$$

where $\eta_n(q)$, $\phi_n(q)$, $\lambda_n(q)$, $\theta_n(q)$ are all real fields. $\lambda_n(q) = \sqrt{2}\eta_n(q)\cos\left[\phi_n(q)\right]$ and $\theta_n(q) = \sqrt{2}\eta_n(q)\sin\left[\phi_n(q)\right]$ can be essentially considered as the amplitude fluctuations and the phase fluctuations, respectively. Then the vector $\Lambda(q) = \left(\Lambda_{A,q}, \Lambda^*_{A,-q}, \Lambda^*_{B,-q}, \Lambda_{B,q}\right)^T$ is

$$\Lambda(q) = \frac{1}{\sqrt{2}}\begin{pmatrix} 1 & i & 0 & 0 \\ 1 & -i & 0 & 0 \\ 0 & 0 & -i & 1 \\ 0 & 0 & i & 1 \end{pmatrix}\chi(q), \tag{22}$$

where $\chi(q) = \left(\ \lambda_A(q)\ \ \theta_A(q)\ \ \theta_B(q)\ \ \lambda_B(q)\ \right)^T$.

Because the low energy excitations are the phase fluctuations, we only focus on the phase fluctuations in the following part. Integrating out the amplitude fluctuations, the effective action of the phase fluctuations is obtained as

$$\bar{S}_{flu}(\theta) = \frac{\beta}{2}\sum_q[(\ \theta_A\ \ \theta_B\ )\Theta(q)\begin{pmatrix}\theta_A \\ \theta_B\end{pmatrix}]. \tag{23}$$

In the static limit $i\upsilon_l \to \upsilon + i0^+$, the collective modes at zero temperature then can be derived numerically from

$$\det\left[\Theta(q)\right] = 0. \tag{24}$$

See the results in Fig.4. From Fig.4, we find that there exists a gapless collective mode corresponding to the Goldstone mode. In addition, due to the two-sublattice

there exists a gapped collective mode corresponding to the Leggett mode. For the weakly coupling case, the Leggett mode lies in the two-quasiparticle continuum and is strongly damped. With increasing the coupling strength U, the two-quasiparticle continuum of the Bogliubov qusiparticles is above the range of the Goldstone mode and the Leggett mode, i.e., the undamped Leggett mode emerges.

VI. O(3) NONLINEAR σ MODEL

However, the RPA approach underestimates the quantum fluctuations of the SF/CDW order in the long-wavelength limit. To derive the quantum fluctuations in the long-wave-length limit, we focus on the low energy physics of the system by using the renormalization-group (RG) approach. Because the amplitude fluctuations always have a large energy gap, we may ignore it and consider the SF/CDW order parameter as an O(3) rotor with fixed length as $\Delta_0/2$.

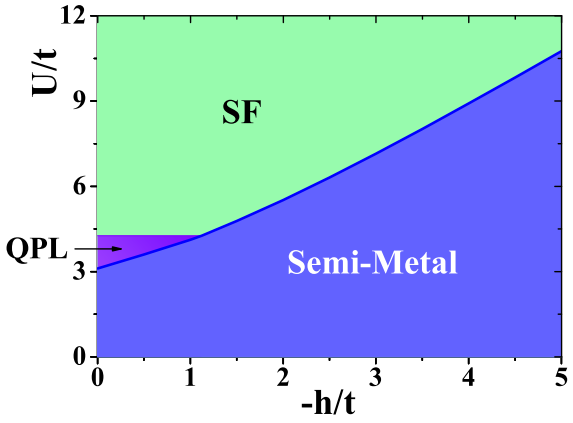

FIG. 5: (Color online) Global phase diagram of attractive π-flux Hubbard model with considering phase fluctuations at zero temperature. There are three phases: semi-metal (blue region), quantum phase liquid (purple region), superfluid (green region).

Now, the effective Lagrangian with spontaneous SU(2) pseudo-spin rotation symmetry breaking under the particle-hole transformation reads

$$\begin{aligned}\mathcal{L}_{\text{eff}} &= \sum_i \tilde{c}_i^\dagger \partial_\tau \tilde{c}_i - \sum_{\langle ij\rangle}(t_{i,j}\tilde{c}_i^\dagger \tilde{c}_j + h.c.) \\ &- \sum_i (-1)^i m_0^{HS} \tilde{c}_i^\dagger \mathbf{\Delta}_i \cdot \sigma \tilde{c}_i - h\sum_i \tilde{c}_i^\dagger \tilde{c}_i.\end{aligned} \tag{25}$$

The SC/CDW order of the attractive Hubbard model corresponds to an antiferromagnetic order of the repulsive Hubbard model, and the quantum phase fluctuations of the attractive Hubbard model correspond to quantum spin fluctuations of the repulsive Hubbard model.

To describe the quantum fluctuations, we use the Haldane's mapping

$$\begin{aligned}\mathbf{\Delta}_i &= (\text{Re}\,\Delta_i, \text{Im}\,\Delta_i, (\rho_i - 1)/2) \\ &= (-1)^i \mathbf{n}_i \Delta_0/2\sqrt{1-\mathbf{L}_i^2} + \mathbf{L}_i,\end{aligned} \tag{26}$$

where $\mathbf{n}_i = (\frac{\text{Re}\,\Delta_i}{\Delta_0/2}, \frac{\text{Im}\,\Delta_i}{\Delta_0/2}, \frac{(-1)^i(\rho_i-1)/2}{\Delta_0/2})$ is the O(3) rotor for the SF/CDW order parameter corresponding to the long wavelength part of $\mathbf{\Delta}_i$ with a restriction $\mathbf{n}_i^2 = 1$, and $\mathbf{L}_i$ is the transverse canting field corresponding to the short wavelength part of $\mathbf{\Delta}_i$ with a restriction $\mathbf{L}_i \cdot \mathbf{n}_i = 0$.

In the long-wave-length limit, after integrating out the fermions and the transverse canting field, the collective modes of the SF/CDW order can be described by the effective O(3) nonlinear σ-model (NLσM)[11, 12]:

$$\mathcal{L}_{\text{SF/CDW}} = \frac{1}{2gv}[(\partial_\tau \mathbf{n})^2 + v^2 (\bigtriangledown \mathbf{n})^2]. \tag{27}$$

Here, the coupling constant g and the collective mode's velocity v are defined as

$$g = \frac{v}{\rho_{\text{phase}}}, \tag{28}$$

and

$$v^2 = \rho_{\text{phase}}[(\frac{1}{4N_s}\sum_{E_{\mathbf{k}}>-h} (m_0^{HS})^2/E_{\mathbf{k}}^{\frac{3}{2}})^{-1} - 2U] \tag{29}$$

where the phase stiffness of the SF order is

$$\rho_{\text{phase}} = \frac{1}{2N_s}\sum_{E_k>-h} \frac{\{(m_0^{HS})^2 + 3t^2 + t^2\cos(4k_x) + \cos(2k_x)\left[8t^2 + 4t^2\cos(2k_y) + (m_0^{HS})^2\right]\}^2}{\left(\xi_k^2 + (m_0^{HS})^2\right)^{\frac{3}{2}}}, \tag{30}$$

and the energy spectrum $E_{\mathbf{k}} = \sqrt{\xi_{\mathbf{k}}^2 + \left(m_0^{HS}\right)^2}$ with $\xi_{\mathbf{k}} = 2t\sqrt{[\cos^2(k_x) + \cos^2(k_y)]}$. See Appendix B for the detailed calculations.

The properties of the effective O(3) NLσM are determined by the dimensionless coupling constant $\alpha = g\Lambda$[13, 14], of which the cutoff is defined as $\Lambda =$

$\min\left(1,\ 2m_0^{HS}/v\right)$. Using the RG approach[13], the RG scaling equation had been obtain as

$$\frac{d\alpha}{dl} = -\alpha + \frac{\alpha^2}{4\pi} \tag{31}$$

where e^l is the length rescaling factor. Particularly, there exists a critical point $\alpha_c = 4\pi$ ($g_c = \frac{4\pi}{\Lambda}$). The quantum critical point separates the long range SF/CDW order and the short range one (the quantum phase liquid). The global phase diagram with considering phase fluctuations of the π-flux attractive Hubbard model is given in Fig.5. From it, we can see that except for the semi-metal phase ($\Delta_0 = 0$) and the SF-CDW phase ($\Delta_0 \neq 0$, $\alpha < 4\pi$), there exists an additional phase ($\Delta_0 \neq 0$, $\alpha > 4\pi$) - quantum phase liquid (the purple region in Fig.5). For the case of $h = 0$, the quantum phase liquid lies between $(U/t)_{c_1} = 3.12$ and $(U/t)_{c_2} = 4.26$. As the Zeeman field strength increases, the QPL region shrinks. For the case of $-h = 0.5t$, the region of the QPL is $(U/t)_{c_1} = 3.60 < U/t < (U/t)_{c_2} = 4.26$. While for $-h > 1.06t$, there doesn't exist the QPL at all.

For the case of $\Delta_0 \neq 0$, $\alpha < 4\pi$, at zero temperature, the interaction between the collective modes is irrelevant ($g(l) \to 0$ for $l \to \infty$) and the ground state has long range SF/CDW order. As shown in Fig.6 (the red line), the order parameter is not zero $\langle \hat{c}^\dagger_{i\uparrow}\hat{c}^\dagger_{i\downarrow}\rangle \neq 0$. However, due to the strong thermal fluctuations, the SF transition temperature is zero. Fig.6 (the blue line) also shows the SF correlation length ξ at $k_BT = 0.02t$ [15]which is really an infinite value for $T \to 0$.

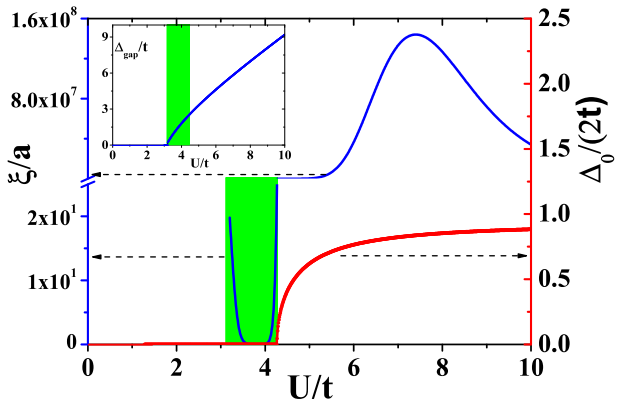

FIG. 6: (Color online) The SF correlation length ξ (the blue line) at $k_BT = 0.02t$ with $h = -0.1t$ and the SF order parameter (the red line) at zero temperature with $h = -0.1t$. The green region is the QPL with short range SF correlation and zero SF order parameter. The inset is the SF energy gap of fermions which is finite in the QPL at zero temperature.

For the case of $\Delta_0 \neq 0$, $\alpha > 4\pi$, the quantum fluctuations are strong enough and the interaction between the collective modes becomes relevant ($g(l) \to \infty$ for $l \to \infty$). Now the ground state turns into QPL. There is no long range SF phase coherence and the SF order parameter is zero, $\langle \hat{c}^\dagger_{i\uparrow}\hat{c}^\dagger_{i\downarrow}\rangle = 0$. Thus in this region, the SF correlation decays exponentially

$$\left\langle \hat{\Delta}^*(x,y)\hat{\Delta}(0)\right\rangle \sim e^{i\mathbf{q}\cdot\mathbf{x}_i}e^{-r/\xi} \tag{32}$$

with $\mathbf{q} = (\pi,\pi)$, $r = \sqrt{x^2+y^2}$. Here ξ is the SF correlation length, $\xi = [4\pi v(\frac{1}{g_c} - \frac{1}{g})]^{-1}$. Then the collective excitations have a mass gap as $4\pi v\left(\frac{1}{g_c} - \frac{1}{g}\right)$ (see the red dotted line in Fig.4, of which a small energy gap of the Goldstone modes appears due to quantum fluctuations). The SF correlation length ξ is a finite value as $T \to 0$. The inset of Fig.6 shows that the energy gap of the paired fermions is always finite in the QPL region.

It is necessary to point out that the QPL corresponds to quantum spin liquid as shown in Fig.8(b) in the repulsive π-flux Hubbard model on square lattice in the intermediate coupling region[16]. The prediction of the quantum spin liquid state near Mott insulator (MI) transition of the repulsive π-flux Hubbard model in Ref.[16] has been confirmed by the quantum Monte-Carlo (QMC) calculation[17].

VII. SUPERFLUID VORTEX

Finally we study the topological excitations in the QPL - the SF vortices. The SF vortex solution is known as

$$\Delta_i = \Delta_0/2\exp\{\pm i\mathrm{Im}[\ln(z_i - z_0)]\phi_i\} \tag{33}$$

where $z \equiv x + iy$ denotes the position of the SF vortex and the subscript i denotes the lattice site. See the illustration in Fig.7(a). In long range SF/CDW order, SF vortex and SF anti-vortex have infinite energy and are all confined. While in the short range SF/CDW order (QPL), the SF vortex and SF anti-vortex have finite energy and are deconfined. Now the SF vortices are true excitations. A question arises "*is the vortex a boson or a fermion*?" To answer this question we study the induced quantum number on the vortex firstly.

From the numerical results, we find that there exist two fermionic zero modes on each SF vortex. Fig.7(b) is the particle-density of the fermionic zero modes around an SF vortex on 55-by-55 lattice by the numerical calculations. As shown in Ref.[18], the existence of the fermionic zero mode leads to an induced pseudo-spin number inside the SF vortex core as $\langle\hat{\eta}^z\rangle = \pm\frac{1}{2}$. According to the mapping from the attractive model to the repulsive model, i.e., $\frac{1}{2}(\rho - 1) \leftrightarrow \hat{\eta}^z$, for $\langle\hat{\eta}^z\rangle = \frac{1}{2}$, we have

$$\left\langle \sum_i \left(\hat{c}^\dagger_{i\uparrow}\hat{c}_{i\uparrow} + \hat{c}^\dagger_{i\downarrow}\hat{c}_{i\downarrow}\right)\right\rangle = 2, \tag{34}$$

which means a pair of fermions inside the SF vortex; for $\langle\hat{\eta}^z\rangle = -\frac{1}{2}$, we have

$$\left\langle \sum_i \left(\hat{c}^\dagger_{i\uparrow}\hat{c}_{i\uparrow} + \hat{c}^\dagger_{i\downarrow}\hat{c}_{i\downarrow}\right)\right\rangle = 0, \tag{35}$$

which means such SF vortex is trivial. See the illustration in Fig.8(a).

In the quantum phase liquid, the superfluid (SF) vortex and the SF anti-vortex have finite energy and are deconfined. Now the SF vortices are true excitations. A question arises "*is the vortex a boson or a fermion*?" Let us answer this question.

Firstly, we calculate the fermion zero modes on the SF vortex by the continuum formula of the effective model in Eq.(B1) in the Appendix B. The SF vortex solution is given in Eq.(33). The size of the vortex core is $\Lambda^{-1} = \max(a, (\Delta_0)^{-1})$. After the particle-hole transformation, the SF vortex of the attractive Hubbard model corresponds to the half-skyrmion of the repulsive Hubbard model as

$$\mathbf{n}_0 = (\frac{x-x_0}{|\mathbf{r}-\mathbf{r}_0|},\ \pm\frac{y-y_0}{|\mathbf{r}-\mathbf{r}_0|},\ 0). \tag{36}$$

In the continuum limit, the effective Lagrangian describes the low energy fermionic excitations at two nodes $\mathbf{k}_1 = (\frac{\pi}{2}, \frac{\pi}{2})$, $\mathbf{k}_2 = (\frac{\pi}{2}, -\frac{\pi}{2})$, and is written as

$$\begin{aligned}\mathcal{L}_{\text{eff}} &= i\bar{\Psi}_1\gamma_\mu\partial_\mu\Psi_1 + i\bar{\Psi}_2\gamma_\mu\partial_\mu\Psi_2 \\ &+ m_0^{HS}(\bar{\Psi}_1\mathbf{n_0}\cdot\sigma\Psi_1 - \bar{\Psi}_2\mathbf{n_0}\cdot\sigma\Psi_2)\end{aligned} \tag{37}$$

where $\Psi_1 = (\ \tilde{c}_{\uparrow 1\mathrm{A}}\ \tilde{c}_{\uparrow 1\mathrm{B}}\ \tilde{c}_{\downarrow 1\mathrm{A}}\ \tilde{c}_{\downarrow 1\mathrm{B}}\ )^T$ and $\Psi_2 = (\ \tilde{c}_{\uparrow 2\mathrm{B}}\ \tilde{c}_{\uparrow 2\mathrm{A}}\ \tilde{c}_{\downarrow 2\mathrm{B}}\ \tilde{c}_{\downarrow 2\mathrm{A}}\ )^T$ with A and B representing sublattices. γ_μ is defined as $\gamma_0 = \sigma_0 \otimes \tau_z$, $\gamma_1 = \sigma_0 \otimes \tau_y$, $\gamma_2 = \sigma_0 \otimes \tau_x$, $\sigma_0 = \begin{pmatrix} 1 & 0 \\ 0 & 1 \end{pmatrix}$. τ^x, τ^y, τ^z are Pauli matrices. We set the Fermi velocity to be unit, i.e., $v_F = 1$. The solutions of zero modes are given by

$$\Psi_1^0(\mathbf{r}) = \begin{pmatrix} 0 \\ \exp(-\frac{|\mathbf{r}-\mathbf{r}_0|}{m_0^{HS}}) \\ \exp(-\frac{|\mathbf{r}-\mathbf{r}_0|}{m_0^{HS}}) \\ 0 \end{pmatrix},\ \Psi_2^0(\mathbf{r}) = \begin{pmatrix} 0 \\ -\exp(-\frac{|\mathbf{r}-\mathbf{r}_0|}{m_0^{HS}}) \\ \exp(-\frac{|\mathbf{r}-\mathbf{r}_0|}{m_0^{HS}}) \\ 0 \end{pmatrix} \tag{38}$$

in Ref.[18]. This result is consistent with that in Fig.7(b) by numerical calculations.

Next, we calculate the induced quantum number on the SF vortex. For the solutions of zero modes, there are four zero-energy soliton states around an SF vortex which are denoted by

$$\begin{aligned} &|\ 1_+\rangle\otimes|\ 2_+\rangle,\quad |\ 1_-\rangle\otimes|\ 2_-\rangle, \\ &|\ 1_-\rangle\otimes|\ 2_+\rangle,\quad |\ 1_+\rangle\otimes|\ 2_-\rangle. \end{aligned} \tag{39}$$

Here $|\ 1_-\rangle$ and $|\ 2_-\rangle$ are empty states of the zero modes $\Psi_1^0(\mathbf{r})$ and $\Psi_2^0(\mathbf{r})$; $|\ 1_+\rangle$ and $|\ 2_+\rangle$ are occupied states of them. At half filling, the soliton states of an SF vortex $|\ \mathrm{sol}\rangle$ are denoted by $|\ 1_-\rangle\otimes|\ 2_+\rangle$ and $|\ 1_+\rangle\otimes|\ 2_-\rangle$. In Ref.[18], the induced quantum numbers of the solitons states including total induced fermion number $\hat{N}_F = \sum_{\alpha,i}\hat{c}_i^\dagger\sigma_z\hat{c}_i$ and the induced staggered spin number $\hat{\eta}^z_{(\pi,\pi)} = \frac{1}{2}\sum_{i\in\mathrm{A}}\tilde{c}_i^\dagger\sigma_z\tilde{c}_i - \frac{1}{2}\sum_{i\in\mathrm{B}}\tilde{c}_i^\dagger\sigma_z\tilde{c}_i$ have been calculated. The total induced fermion number on the solitons is zero due to the cancelation effect between two nodes, i.e., $\hat{N}_F\ |\ \mathrm{sol}\rangle = 0$. However, there exists an induced staggered pseudo-spin moment on the soliton states[18],

$$\hat{\eta}^z_{(\pi,\pi)}\ |\ \mathrm{sol}\rangle = \pm\frac{1}{2}\ |\ \mathrm{sol}\rangle. \tag{40}$$

From the fact of $\mathbf{n}_i = \bar{\mathbf{z}}_i\sigma\mathbf{z}_i$ where $\mathbf{z}$ is a bosonic spinon, $\mathbf{z} = (z_1, z_2)$ and $\bar{\mathbf{z}}\mathbf{z} = \mathbf{1}$, the induced staggered spin number on a SF vortex means that there exists a trapped bosonic spinon inside the vortex-core. On the other hand,

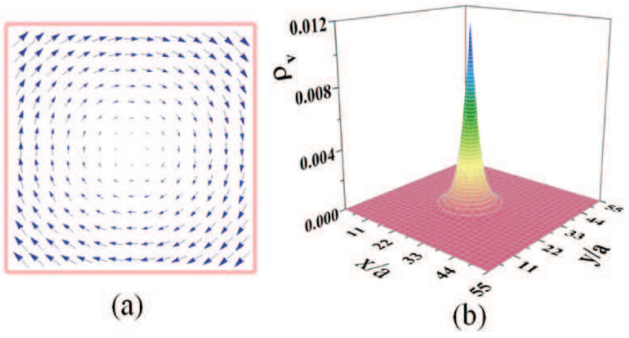

FIG. 7: (Color online) (a) The illustration of an SF vortex. (b) The particle-density ρ_v of the fermionic zero modes around an SF vortex on 55-by-55 lattice. We take the case of $U = 3.5t$, $\Delta_0 = 0.25$, $h = 0.0$ as an example.

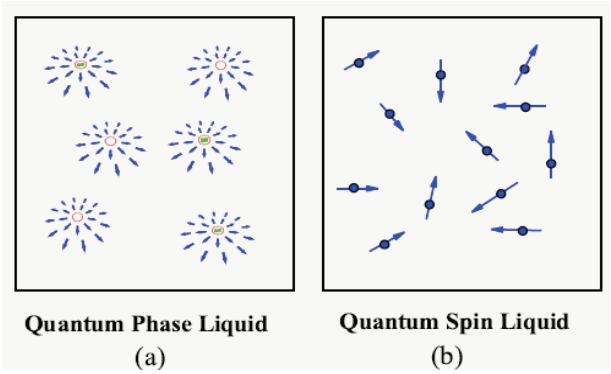

FIG. 8: (Color online) The illustration of the quantum phase liquid (QPL) and quantum spin liquid (QSL): (a) The elemental excitations of QPL are the two-component fermionic SF vortices (or anti-vortices) with or without a Cooper pair inside the vortex core. Two green spots denote a Cooper pair; (b) The elemental excitations of the QSL are the spinons.

the O(3) nonlinear σ model is equivalent to CP(1) model

$$\begin{aligned}\mathcal{L}_{\mathbf{s}} &= \frac{1}{2gv}[(\partial_\tau\mathbf{n})^2 + v^2\,(\bigtriangledown\mathbf{n})^2] \\ &= \frac{2}{gv}[|(\partial_\tau - ia_\tau)\mathbf{z}|^2 + v^2|(\vec{\nabla} - i\vec{a})\mathbf{z}|^2]\end{aligned} \tag{41}$$

where $a_\mu \equiv -\frac{i}{2}(\bar{\mathbf{z}}\partial_\mu\mathbf{z} - \partial_\mu\bar{\mathbf{z}}\mathbf{z})$ is introduced as an auxiliary gauge field. That means the bosonic spinon $\mathbf{z}$ carries a

unit charge of the auxiliary gauge field a_μ. When the bosonic spinon $\mathbf{z}$ moves around an SF vortex, its wavefunction will obtain an extra minus sign. The SF vortex is really a π-flux of the bosonic spinon $\mathbf{z}$. Hence, due to the mutual semion statistics between the bosonic spinon $\mathbf{z}$ and the SF vortex, a mobile SF vortex trapping a bosonic spinon $\mathbf{z}$ becomes a composite fermionic particle. We call such composite object (fermion with $\pm\frac{1}{2}$ pseudo-spin degree freedom) a "*fermionic SF vortex*"[18].

Then, if there is no magnetic flux, i.e., $B = 0$, the density of the fermionic SF vortices is zero at zero temperature. When we apply the extra magnetic field, $B \neq 0$ (or away from the π-flux case slightly), the density of the fermionic SF vortices becomes finite[19]. In conventional SFs with external magnetic field, below the Kosterlitz-Thouless (KT) transition temperature, people can observe a vortex-lattice; While above the KT transition temperature, the vortex-lattice will melt and the (bosonic) vortices will move randomly. In the QPL, because each quantized magnetic flux turns into a fermionic SF vortex, there is a dilute fermionic-SF-vortex gas that forms a Fermi liquid for the weak magnetic field case. The fermionic vortex density is determined by the external field $n_v^0 = B/\phi_0$ with ϕ_0 being the quantized flux. Now the ground state of the attractive π-flux Hubbard model becomes a QPL with vortex-Fermi-surface, which leads to quite un-usual physical consequences. People may use the time-of-flight approach to observe the signature of Fermi liquid of vortices.

VIII. CONCLUSION

In this paper, based on timely technique, we point out that the realization of a π-flux model in a square optical lattice of cold atoms provides an opportunity to get a new type of quantum fluid. From an attractive π-flux Hubbard model, we have an SF/CDW order from spontaneous SU(2) pseudo-spin rotation symmetry breaking. Due to fairly strong quantum fluctuations, there may exist a possible quantum phase liquid state, in which there exists Cooper pairing, but no long range SF phase coherence exists. In addition, we may even guess that in different SFs with SU(2) particle-hole symmetry there may exist different types of quantum phase liquids with different types of SF vortices. This issue will be explored in a future study.

Finally, we discuss the possible experimental signatures of QPL. The QPL is a short range quantum SF order. In QPL, the SF correlation decays exponentially as $\left\langle \hat{\Delta}^*(x,y)\hat{\Delta}(0)\right\rangle \sim e^{i\mathbf{q}\cdot\mathbf{x}_i}\exp\{-[4\pi v(\frac{1}{g_c}-\frac{1}{g})]r\}$ with $\mathbf{q} = (\pi,\pi)$. Thus, people may detect the pairing correlation to observe the QPL. In particular, the fermionic SF vortex in QPL has different topological properties from the SF vortex in the systems with pseudo-energy-gap at finite temperature, of which the SF vortex always obeys bosonic statistics. The QPL with finite vortex-density forms a vortex-metal with Fermi-surface. The Fermi-surface of cold fermions in a 3D optical lattice has been successfully observed[20]. Similarly, one may also observe these Fermi levels of SF-vortices in this system. In addition, even in long range SF order (the green region in Fig.5), the SF vortex has the same fermionic zero modes as that in QPL order. People may directly observe the fermionic zero modes on the SF vortices by time-of-flight imaging in a long range SF order.

Acknowledgments

The authors thank H. Zhai and R. Q. Wang for helpful discussions. This work is supported by National Basic Research Program of China (973 Program) under the grant No. 2011CB921803, 2012CB921704, NSFC Grant No. 11174035.

Appendix A: Mapping attractive model to repulsive model

In the Landau gauge, the explicit form of kinetic term of the π-flux attractive Hubbard model shown in Eq.(3) takes the form

$$\begin{aligned}\hat{H}_K^L = &-\sum_{i,\sigma} t\left(\hat{c}^\dagger_{i,\sigma}\hat{c}_{i+e_x,\sigma} + \hat{c}^\dagger_{i,\sigma}\hat{c}_{i-e_x,\sigma}\right)\\ &-\sum_{i,\sigma}\left[(-1)^{i_x}\,\hat{c}^\dagger_{i,\sigma}\hat{c}_{i+e_y,\sigma} + (-1)^{i_x}\,\hat{c}^\dagger_{i,\sigma}\hat{c}_{i-e_y,\sigma}\right].\end{aligned} \tag{A1}$$

By the particle-hole transformation $\hat{c}_{i,\uparrow} \to \tilde{c}_{i,\uparrow}$, $\hat{c}^\dagger_{i,\uparrow} \to \tilde{c}^\dagger_{i,\uparrow}$, $\hat{c}_{i,\downarrow} \to (-1)^{i_x+i_y}\,\tilde{c}^\dagger_{i,\downarrow}$, $\hat{c}^\dagger_{i,\downarrow} \to (-1)^{i_x+i_y}\,\tilde{c}_{i,\downarrow}$, one may map the attractive Hubbard model to a repulsive Hubbard model.

The kinetic term becomes

$$\begin{aligned}\hat{H}_K^L \to &-\sum_i t\left(\tilde{c}^\dagger_{i,\uparrow}\tilde{c}_{i+e_x,\uparrow} + \tilde{c}^\dagger_{i,\uparrow}\tilde{c}_{i-e_x,\uparrow}\right)\\ &-\sum_i t\left((-1)^{i_x}\,\tilde{c}^\dagger_{i,\uparrow}\tilde{c}_{i+e_y,\uparrow} + (-1)^{i_x}\,\tilde{c}^\dagger_{i,\uparrow}\tilde{c}_{i-e_y,\uparrow}\right)\\ &-\sum_i t\left(\tilde{c}^\dagger_{i+e_x,\downarrow}\tilde{c}_{i,\downarrow} + \tilde{c}^\dagger_{i-e_x,\downarrow}\tilde{c}_{i,\downarrow}\right)\\ &-\sum_i t\left((-1)^{i_x}\,\tilde{c}^\dagger_{i+e_y,\downarrow}\tilde{c}_{i,\downarrow} + (-1)^{i_x}\,\tilde{c}^\dagger_{i-e_y,\downarrow}\tilde{c}_{i,\downarrow}\right)\\ &= \tilde{H}_K^L;\end{aligned} \tag{A2}$$

The on-site interaction term becomes

$$\hat{H}_U^L \to U\sum_i \tilde{n}_{i,\uparrow}\tilde{n}_{i,\downarrow} - U\sum_i \tilde{n}_{i,\uparrow}; \tag{A3}$$

The chemical potential term becomes

$$\hat{H}_\mu^L \to -\mu\sum_{i,\sigma}\left(\tilde{c}^\dagger_{i,\uparrow}\tilde{c}_{i,\uparrow} - \tilde{c}^\dagger_{i,\downarrow}\tilde{c}_{i,\downarrow}\right) - \mu N; \tag{A4}$$

The Zeeman field term becomes

$$\hat{H}_Z^L \to -h\sum_i \left(\tilde{c}_{i,\uparrow}^\dagger \tilde{c}_{i,\uparrow} + \tilde{c}_{i,\downarrow}^\dagger \tilde{c}_{i,\downarrow}\right) + hN. \tag{A5}$$

In summary, the Hamiltonian of the π-flux attractive Hubbard model under the particle-hole transformation turns into

$$\begin{aligned}\hat{H} \to \tilde{H} = \tilde{H}_K^L + U\sum_i \tilde{n}_{i,\uparrow}\tilde{n}_{i,\downarrow} - \tilde{h}\sum_{i,\sigma,\sigma'} \tilde{c}_{i\sigma}^\dagger \sigma_{\sigma\sigma'}^z \tilde{c}_{i\sigma'} \\ - \tilde{\mu}\sum_{i,\sigma} \tilde{n}_{i,\sigma} - \mu N + hN,\end{aligned} \tag{A6}$$

where the effective Zeeman field and the effective chemical potential are given by $\tilde{h} = \mu + \frac{U}{2}$ and $\tilde{\mu} = \frac{U}{2} + h$, respectively. In the followings, we neglect the constant $-\mu N + hN$, and arrive at the form of the repulsive Hubbard model as

$$\tilde{H} = \tilde{H}_K^L + U\sum_i \tilde{n}_{i,\uparrow}\tilde{n}_{i,\downarrow} - \tilde{\mu}\sum_{i,\sigma} \tilde{n}_{i,\sigma}. \tag{A7}$$

The order parameters under the particle-hole transformation turns into

$$\begin{aligned}\Delta_i &= \hat{c}_{i,\uparrow}^\dagger \hat{c}_{i,\downarrow}^\dagger \to \tilde{c}_{i,\uparrow}^\dagger (-1)^i \tilde{c}_{i,\downarrow} \\ &= (-1)^i \hat{\eta}_i^-, \end{aligned} \tag{A8}$$

$$\Delta_i^\dagger = \hat{c}_{i,\downarrow}\hat{c}_{i,\uparrow} \to (-1)^i \hat{\eta}_i^+ \tag{A9}$$

$$\begin{aligned}\rho_i &= \hat{c}_{i,\uparrow}^\dagger \hat{c}_{i,\uparrow} + \hat{c}_{i,\downarrow}^\dagger \hat{c}_{i,\downarrow} \\ &\to \tilde{c}_{i,\uparrow}^\dagger \tilde{c}_{i,\uparrow} - \tilde{c}_{i,\downarrow}^\dagger \tilde{c}_{i,\downarrow} + 1 \\ &= 2\hat{\eta}_i^z + 1, \end{aligned} \tag{A10}$$

with $\hat{\eta}^\pm = \hat{\eta}_x \pm i\hat{\eta}_y$, where the pseudo-spin operators are $\hat{\eta}_\gamma = \tilde{c}_\alpha^\dagger \sigma_{\alpha,\beta}^\gamma \tilde{c}_\beta/2$, in which σ^γ are Pauli matrices with $\gamma = x, y, z$. In conclusion, we have the relationship between attractive Hubbard model and repulsive Hubbard model as follows:

Attractive interaction	Repulsive interaction
$(-1)^i \Delta_i$	$\hat{\eta}_i^-$
$(-1)^i \Delta_i^\dagger$	$\hat{\eta}_i^+$
$\frac{1}{2}(\rho_i - 1)$	$\hat{\eta}_i^z$

Appendix B: Effective Nonlinear σ Model of SF/CDW order

To study the quantum fluctuations of the SC/CDW order, we get an effective Lagrangian with spontaneous SU(2) pseudo-spin rotation symmetry breaking under the particle-hole transformation as

$$\begin{aligned}\mathcal{L}_{\text{eff}} = \sum_i \tilde{c}_i^\dagger \partial_\tau \tilde{c}_i - \sum_{\langle ij\rangle}(t_{i,j}\tilde{c}_i^\dagger \tilde{c}_j + h.c.) \\ - \sum_i (-1)^i m_0^{HS} \tilde{c}_i^\dagger \mathbf{\Delta}_i \cdot \sigma \tilde{c}_i - h\sum_i \tilde{c}_i^\dagger \tilde{c}_i.\end{aligned} \tag{B1}$$

To describe the quantum fluctuations, we use the Haldane's mapping:

$$\begin{aligned}\mathbf{\Delta}_i &= (\text{Re}\,\Delta_i, \text{Im}\,\Delta_i, (\rho_i - 1)/2) \\ &= (-1)^i \mathbf{n}_i \Delta_0/2\sqrt{1 - \mathbf{L}_i^2} + \mathbf{L}_i, \end{aligned} \tag{B2}$$

where $\mathbf{n}_i = (\frac{\text{Re}\,\Delta_i}{\Delta_0/2}, \frac{\text{Im}\,\Delta_i}{\Delta_0/2}, \frac{(-1)^i(\rho_i - 1)/2}{\Delta_0/2})$ is the O(3) rotor for the SF/CDW order parameter, which refers to the long wavelength part of $\mathbf{\Delta}_i$ with a restriction $\mathbf{n}_i^2 = 1$, and $\mathbf{L}_i$ is the transverse canting field corresponding to the short wavelength part of $\mathbf{\Delta}_i$ with a restriction $\mathbf{L}_i \cdot \mathbf{n}_i = 0$.

We then rotate $\mathbf{\Delta}_i$ to the $\hat{\mathbf{z}}$-axis by performing the following transformation:

$$\begin{aligned}\Psi_i &= U_i^\dagger \tilde{c}_i, \\ U_i^\dagger \mathbf{n}_i . \sigma U_i &= \sigma_z, \\ U_i^\dagger \mathbf{L}_i . \sigma U_i &= \mathbf{l}_i . \sigma, \end{aligned} \tag{B3}$$

where $U_i \in \text{SU(2)/U(1)}$. One then can derive the following effective Lagrangian:

$$\begin{aligned}\mathcal{L}_{\text{eff}} = \sum_i \Psi_i^\dagger \left[\partial_\tau + \left(U_i^\dagger \partial_\tau U_i\right) - h\right] \Psi_i \\ - \sum_{\langle i,j\rangle} \left(t_{ij}\Psi_i^\dagger e^{ia_{ij}} \Psi_j + h.c.\right) \\ - m_0^{HS} \sum_i \Psi_i^\dagger \left[(-1)^i \sigma_z \sqrt{1 - \mathbf{l}_i^2} + \mathbf{l}_i . \sigma\right] \Psi_i,\end{aligned} \tag{B4}$$

where $m_0^{HS} = U\Delta_0/2$, the auxiliary gauge fields $a_{ij} = a_{ij,1}\sigma_x + a_{ij,2}\sigma_y$, and $a_0(i) = a_{0,1}(i)\sigma_x + a_{0,2}(i)\sigma_y$ are defined as

$$\begin{aligned}e^{ia_{ij}} &= U_i^\dagger U_j, \\ a_0(i) &= U_i^\dagger \partial_\tau U_i. \end{aligned} \tag{B5}$$

By means of the mean field result $\Delta_0/2 = (-1)^i \left\langle \Psi_i^\dagger \sigma_z \Psi_i \right\rangle$ and the approximations

$$\begin{aligned}\sqrt{1 - \mathbf{l}_i^2} &\simeq 1 - \frac{\mathbf{l}_i^2}{2}, \\ e^{ia_{ij}} &\simeq 1 + ia_{ij}, \end{aligned} \tag{B6}$$

we obtain

$$\begin{aligned}\mathcal{L}_{\text{eff}} = \sum_i \Psi_i^\dagger \left[\partial_\tau + a_0(i) - m_0^{HS}\left(\mathbf{l}_i . \sigma + (-1)^i \sigma_z\right) - h\right] \Psi_i \\ - \sum_{\langle ij\rangle} \left[t_{ij}\Psi_i^\dagger (1 + ia_{ij}) \Psi_j + h.c.\right] + m_0^{HS} \sum_i \frac{\mathbf{l}_i^2}{2}.\end{aligned} \tag{B7}$$

Performing integration out the fermion field, we then get the effective action

$$\begin{aligned}\mathcal{S}_{\text{eff}} = \frac{1}{2}\int_0^\beta d\tau \sum_i \left[-4\varsigma \left(a_0(i) - m_0^{HS}\mathbf{l}_i . \sigma - h\right)^2 + 4\rho_{\text{phase}} a_{ij}^2\right] \\ + \frac{1}{2}\int_0^\beta d\tau \sum_i \frac{2\left(m_0^{HS}\right)^2}{U}\mathbf{l}_i^2,\end{aligned} \tag{B8}$$

where ς and ρ_{phase} (the phase stiffness) are two parameters. Next, to learn the properties of the low energy physics, we study the continuum theory of the effective action in Eq.(B8). In the continuum limit, we denote the quantities $\mathbf{n}_i \to \mathbf{n}(x,y)$, $\mathbf{l}_i \to \mathbf{l}(x,y)$, $ia_{ij} = U_i^\dagger U_j - 1 \to U^\dagger \partial_\mu U$ ($\mu = x$ or y), $U_i^\dagger \partial_\tau U_i \to U^\dagger \partial_\tau U$, respectively. From the relations between $U^\dagger \partial_\mu U$ and $\partial_\mu \mathbf{n}$, we obtain

$$\begin{aligned} a_\tau^2 &= a_{\tau,1}^2 + a_{\tau,2}^2 = -\frac{1}{4}\left(\partial_\tau \mathbf{n}\right)^2, \\ a_\mu^2 &= a_{\mu,1}^2 + a_{\mu,2}^2 = \frac{1}{4}\left(\partial_\mu \mathbf{n}\right)^2, \mu = x, y, \\ \mathbf{a}_0.\mathbf{l} &= -\frac{i}{2}\left(\mathbf{n} \times \partial_\tau \mathbf{n}\right).\mathbf{l}, \end{aligned} \tag{B9}$$

where 1, 2 denote the two spin flavors. We then integrate out the transverse canting field $\mathbf{l}$ and obtain the effective action as follows:

$$\mathcal{S}_{\text{eff}} = \frac{\rho_{\text{phase}}}{2}\int_0^\beta d\tau \int d^2 r \left[\left(\bigtriangledown \mathbf{n}\right)^2 + \frac{1}{v^2}\left(\partial_\tau \mathbf{n}\right)^2\right] + S_B\left[\mathbf{n}\right], \tag{B10}$$

where $v = \sqrt{\rho_{\text{phase}}\left(1/\varsigma - 2U\right)}$ and $S_B\left[\mathbf{n}\right]$ are other terms which are irrelevant to the second order term about vector **n.**

To give the coefficients ς and ρ_s, we choose U_i in CP(1) representation to be

$$U_i = \begin{pmatrix} z_{i\uparrow}^* & z_{i\downarrow}^* \\ -z_{i\downarrow} & z_{i\uparrow} \end{pmatrix}, \tag{B11}$$

where $\mathbf{z}_i = \left(z_{i\uparrow}, z_{i\downarrow}\right)^T$, $\bar{\mathbf{z}}_i \mathbf{z}_i = 1$, and $\mathbf{n}_i = \bar{\mathbf{z}}_i \sigma \mathbf{z}_i$ [21]. The quantum fluctuations around $\mathbf{n}_i = \hat{\mathbf{z}}_i$ is

$$\begin{aligned} \mathbf{n}_i &= \hat{\mathbf{z}}_i + \mathrm{Re}\left(\phi_i\right)\hat{\mathbf{x}}_i + \mathrm{Im}\left(\phi_i\right)\hat{\mathbf{y}}_i, \\ \hat{\mathbf{z}}_i &= \begin{pmatrix} 1 - \frac{|\phi_i|^2}{8} \\ \frac{\phi_i}{2} \end{pmatrix} + O\left(\phi_i^3\right). \end{aligned} \tag{B12}$$

Then the quantities $U_i^\dagger U_j$ and $U_i^\dagger \partial_\tau U_i$ can be expanded in the power of $\phi_i - \phi_j$ and $\partial_\tau \phi_i$, i.e.,

$$\begin{aligned} U_i^\dagger U_j &= e^{-\frac{i}{2}(\phi_i - \phi_j)\sigma_y}, \\ U_i^\dagger \partial\tau U_i &= \begin{pmatrix} 0 & \frac{1}{2}\partial_\tau \phi_i \\ -\frac{1}{2}\partial_\tau \phi_i & 0 \end{pmatrix}. \end{aligned} \tag{B13}$$

The gauge field a_{ij} and $a_0(i)$ are therefore given by

$$\begin{aligned} a_{ij} &= -\frac{i}{2}\left(\phi_i - \phi_j\right), \\ a_0\left(i\right) &= -\frac{i}{2}\partial_\tau \phi_i. \end{aligned} \tag{B14}$$

Assuming that a_{ij} and $a_0(i)$ are constant in space and denoting $\partial_i \phi_i = \mathbf{a}$, and $\partial_\tau \phi_i = iB_y$, we get

$$\begin{aligned} a_{ij} &= -\frac{1}{2}\mathbf{a}.\left(\mathbf{i} - \mathbf{j}\right)\sigma_y, \\ a_0(i) &= -\frac{1}{2}B_y \sigma_y. \end{aligned} \tag{B15}$$

The energy of Hamiltonian of Eq.(B8) becomes

$$E\left(B_y, \mathbf{a}\right) = -\frac{1}{2}\varsigma B_y^2 + \frac{1}{2}\rho_{\text{phase}}\mathbf{a}^2. \tag{B16}$$

Then one may obtain ς and ρ_{phase} by the partial derivative of the energy

$$\begin{aligned} \varsigma &= -\frac{1}{N}\frac{\partial^2 E_0\left(B_y\right)}{\partial B_y^2}\Big|_{B_y=0}, \\ \rho_{\text{phase}} &= \frac{1}{N}\frac{\partial^2 E_0\left(\mathbf{a}\right)}{\partial \mathbf{a}^2}\Big|_{\mathbf{a}=0}, \end{aligned} \tag{B17}$$

where $N = 2N_s$. Here $E_0(B_y)$ and $E_0\left(\mathbf{a}\right)$ are the energy spectra of the lower Hubbard band

$$\begin{aligned} E_0(B_y) &= \sum_{\mathbf{k}}\left(E_{+,\mathbf{k}}^\varsigma + E_{-,\mathbf{k}}^\varsigma\right), \\ E_0(\mathbf{a}) &= \sum_{\mathbf{k}}\left(E_{+,\mathbf{k}}^{\rho_{\text{phase}}} + E_{-,\mathbf{k}}^{\rho_{\text{phase}}}\right), \end{aligned} \tag{B18}$$

where $E_{+,\mathbf{k}}^\varsigma$, $E_{-,\mathbf{k}}^\varsigma$ and $E_{+,\mathbf{k}}^{\rho_{\text{phase}}}$, $E_{-,\mathbf{k}}^{\rho_{\text{phase}}}$ are the energy spectra of the following Hamiltonian H^ς and $H^{\rho_{\text{phase}}}$ given by

$$\begin{aligned} H^\varsigma = &-\sum_{\langle i,j\rangle}\left(t_{ij}\Psi_i^\dagger \Psi_j + h.c.\right) - m_0^{HS}\sum_i \Psi_i^\dagger\left(-1\right)^i \sigma_z \Psi_i \\ &-\sum_i \frac{B_y}{2}\Psi_i^\dagger \sigma_y \Psi_i - h\sum_i \Psi_i^\dagger \Psi_i, \end{aligned} \tag{B19}$$

$$\begin{aligned} H^{\rho_{\text{phase}}} = &-\sum_{\langle i,j\rangle}\left(t_{ij}\Psi_i^\dagger e^{ia_{ij}}\Psi_j + h.c.\right) - h\sum_i \Psi_i^\dagger \Psi_i \\ &- m_0^{HS}\sum_i \Psi_i^\dagger\left(-1\right)^i \sigma_z \Psi_i, \end{aligned} \tag{B20}$$

where $a_{ij} = \frac{1}{2}\left(\mathbf{i} - \mathbf{j}\right)\cdot\sigma$.

By the Fourier transformation for H^ς, we get the spectra of H^ς:

$$E_{\pm,\mathbf{k}}^\varsigma = -\sqrt{\left(\left|\xi_k\right| \pm \frac{B_y}{2}\right)^2 + \left(m_0^{HS}\right)^2}. \tag{B21}$$

Making use of $\varsigma = -\frac{1}{N}\frac{\partial^2 E_0(B_y)}{\partial B_y^2}\Big|_{B_y=0}$, and $E_0\left(B_y\right) = \sum_{\mathbf{k}}\left(E_{+,\mathbf{k}}^\varsigma + E_{-,\mathbf{k}}^\varsigma\right)$, we can obtain

$$\varsigma = \frac{1}{4N_s}\sum_{E_{\mathbf{k}}>-h}\frac{\left(m_0^{HS}\right)^2}{\left(\left|\xi_k\right|^2 + \Delta^2\right)^{\frac{3}{2}}}. \tag{B22}$$

Similarly, we can get energy spectra of $H^{\rho_{\text{phase}}}$:

$$E_{\pm,\mathbf{k}}^{\rho_{\text{phase}}} = -\sqrt{P_x^2 + P_y^2 + Q_x^2 + Q_y^2 \pm 2f}, \tag{B23}$$

where

$$
\begin{aligned}
f &= \sqrt{\Delta^2\left(Q_x^2+Q_y^2\right)+\left(P_xQ_x+P_yQ_y\right)^2},\\
P_x &= 2t\cos\left(\frac{a_x}{2}\right)\cos k_x,\\
P_y &= 2t\cos\left(\frac{a_y}{2}\right)\cos k_y,\\
Q_x &= 2t\sin\left(\frac{a_x}{2}\right)\sin k_x,\\
P_y &= 2t\sin\left(\frac{a_y}{2}\right)\sin k_y.
\end{aligned}
\tag{B24}
$$

Finally, we derive the effective O(3) nonlinear σ-model (NLσM):

$$
\mathcal{L}_{\mathrm{SF/CDW}} = \frac{1}{2g}[\left(\partial_\tau \mathbf{n}\right)^2 + \frac{1}{v^2}\left(\bigtriangledown \mathbf{n}\right)^2]. \tag{B25}
$$

The coupling constant g and the collective mode's velocity v are defined as

$$
\begin{aligned}
g &= \frac{v}{\rho_{\mathrm{phase}}},\\
v^2 &= \rho_{\mathrm{phase}}[(\frac{1}{4N_s}\sum_{E_{\mathbf{k}}>-h}\frac{(m_0^{HS})^2}{E_{\mathbf{k}}^{\frac{3}{2}}})^{-1} - 2U]
\end{aligned}
\tag{B26}
$$

where $m_0^{HS} = U\Delta_0/2$, and the phase stiffness ρ_{phase} of the SF order is shown in Eq.(30) in the main text.

[1] I. Bloch, J. Dalibard and W. Zwerger, Rev. Mod. Phys. **80**, 885 (2008).
[2] S. Giorgini, L. P. Pitaevskii and S. Stringari, Rev. Mod. Phys. **80**, 1215 (2008).
[3] T. Köhler, K. Góral, and P. S. Julienne, Rev. Mod. Phys. **78**, 1311-1361 (2006).
[4] C. Chin, R. Grimm, P. Julienne and E. Tiesinga, Rev. Mod. Phys. **82**, 1225-1286 (2010).
[5] M. Aidelsburger, M. Atala, S. Nascimbène, S. Trotzky, Y.-A. Chen, and I. Bloch, Phys. Rev. Lett. **107,** 255301 (2011).
[6] M. Aidelsburger, M. Atala, M. Lohse, J. T. Barreiro, B. Paredes, I. Bloch, Phys. Rev. Lett. **111**, 185301 (2013).
[7] H. Miyake, G. A. Siviloglou, C. J. Kennedy, W. Cody Burton, W. Ketterle, Phys. Rev. Lett. **111**, 185302 (2013).
[8] Hui Zhai, R.O. Umucahlar, and M.Ö. Oktel, Phys. Rev. Lett. **104**, 145301 (2010).
[9] C. N. Yang and S. C. Zhang, Mod. Phys. Lett. **B 4,** 759 (1990).
[10] M. Iskin and C. A. R. Sá de Melo, Phys. Rev. B **72**, 024512 (2005).
[11] F. D. M. Haldane, Phys. Rev. Lett. **61**, 2015 (1988).
[12] N. Dupuis, Phys. Rev. **B 70**, 134502 (2004).
[13] S. Chakravarty, Bertrand I. Halperin and David R. Nelson, Phys. Rev. B **39**, 2344 (1989).
[14] S. Sachdev, *Quantum Phase Transitions*, (Cambridge University Press, 1999).
[15] In current experiment, for example, according to parameters from Ref.[5], the order of $k_BT = 0.02t$ is about nK. This low-temperature-condition is still a challenge for the fermionic system.
[16] G. Y. Sun and S. P. Kou, EPL, **87,** 67002 (2009).
[17] C. C. Chang and R. T. Scalettar, Phys. Rev. Lett. **109**, 026404 (2012).
[18] S. P. Kou, Phys. Rev. **B 78**, 233104 (2008).
[19] The QPL is a gapped state. Thus, the properties are robust to the perturbations. The small variation of the (uniform) π-flux will cause additional fermionic SF-vortices. If there exists a small extra magnetic field away from the magnetic field in π-flux case, the density of the fermionic SF vortices becomes finite. When the extra magnetic field is far away from the magnetic field in π-flux case, the femionic system has different magnetic translation symmetry and different mean field ansatz. So, in this paper, we only consider the case of magnetic field away from that in π-flux case slightly.
[20] M. Köhl, H. Moritz, T. Stöferle, K. Günter and T. Esslinger, Phys. Rev. Lett. **94**, 080403 (2005).
[21] X. G. Wen, Quantum Field Theory of Many-Body Systems (Oxford Univ. Press, Oxford, 2004).